

for the electrosyntheses of *trans*-[Mo₂Cp₂(CO)₂(μ-SMe)₂] and of [Mo₂Cp₂(CO)(CNR)(μ-SMe)₂] were as described below.

***trans*-[Mo₂Cp₂(CO)₂(μ-SMe)₂].** A solution of complex 1 in a thf–0.2 M [Bu₄N][PF₆] or a MeCN–0.1 M [Bu₄N][PF₆] electrolyte was reduced on a Hg-pool cathode at –1.6 V under N₂ or Ar. The initial dark orange solution turned brown as the experiment proceeded. When the cell current had decayed to the background level, the catholyte was syringed out of the electrochemical cell, transferred into a Schlenk flask under N₂, and taken down to dryness. The residue (product + supporting electrolyte) was extracted four times with ca. 10 mL of pentane, the filtrates were collected in a flask, and the solvent was removed under vacuum. ¹H NMR analysis of the crude product showed the presence of *trans*-[Mo₂Cp₂(CO)₂(μ-SMe)₂] and of trace amounts of supporting electrolyte. The mass spectrum showed ions corresponding to [M]⁺ (*m/e* 472), [M – CO]⁺ (*m/e* 444), [M – 2CO]⁺ (*m/e* 416), [M – 2CO – 2(CH₃)]⁺ (*m/e* 386), [M – 2CO – 2(CH₃) – C₅H₅]⁺ (*m/e* 321), and [M – 2CO – 2(CH₃) – 2(C₅H₅)]⁺ (*m/e* 256).

[Mo₂Cp₂(CO)(CNR)(μ-SMe)₂]. The same procedure as described above was followed, except that isocyanide RNC (R = xyl, 1 equiv; R = Bz, 2 equiv; R = *t*-Bu, 5 equiv) was added to the solution of complex 1. After the workup of the brown to greenish brown catholyte, ¹H NMR spectroscopy showed the presence of two isomers of the product. Column chromatography on silica gel or Florisil did not allow a proper separation of the isomers, which also underwent some decomposition on the column. In order to favor the formation of isomer 1, a vigorous bubbling of

N₂ was maintained through the solution of complex 1 and RNC while the electrolysis was proceeding (see Results). A green solution resulted from the experiments performed under these conditions. After a workup similar to that described for *trans*-[Mo₂Cp₂(CO)₂(μ-SMe)₂], ¹H NMR analysis of the product showed that the ratio of isomer 1 to isomer 2 had increased, with a maximum of 3/1.

R = xyl. Anal. Calcd for [Mo₂Cp₂(CO)(CNxyl)(μ-SMe)₂]. CH₂Cl₂ (Mo₂C₂₃H₂₇NS₂OCl₂): C, 41.8; H, 4.1; N, 2.1; Mo, 29.1. Found: C, 41.5; H, 4.6; N, 2.2; Mo, 29.8. The mass spectrum showed ions corresponding to [M]⁺ (*m/e* 575), [M – (CH₃)]⁺ (*m/e* 560), [M – (CH₃) – (CO)]⁺ (*m/e* 532), [M – (CO) – (xylNC)]⁺ (*m/e* 416), [M – (CO) – (xylNC) – 2(CH₃)]⁺ (*m/e* 386), [M – (CO) – (xylNC) – 2(CH₃) – (C₅H₅)]⁺ (*m/e* 321), and [M – (CO) – (xylNC) – 2(CH₃) – 2(C₅H₅)]⁺ (*m/e* 256).

R = *t*-Bu. The mass spectrum showed ions corresponding to [M]⁺ (*m/e* 527), [M – (CO)]⁺ (*m/e* 499), [M – (*t*-Bu)]⁺ (*m/e* 470), [M – (CO) – (*t*-BuNC)]⁺ (*m/e* 416), [M – (CO) – (*t*-BuNC) – (CH₃)]⁺ (*m/e* 401), [M – (CO) – (*t*-BuNC) – 2(CH₃)]⁺ (*m/e* 386), [M – (CO) – (*t*-BuNC) – 2(CH₃) – (C₅H₅)]⁺ (*m/e* 321), [M – (CO) – (*t*-BuNC) – 2(CH₃) – 2(C₅H₅)]⁺ (*m/e* 256).

R = BzNC. The mass spectrum showed peaks corresponding to [M]⁺ (*m/e* 561), [M – (CO)]⁺ (*m/e* 533), [M – (BzNC)]⁺ (*m/e* 444), and [M – (CO) – (BzNC) – 2(CH₃)]⁺ (*m/e* 386).

Acknowledgment. The CNRS (Centre National de la Recherche Scientifique) is acknowledged for financial support to this work.

Crystal and Molecular Structure of an Asymmetric Hydrogenation Catalyst–Substrate Adduct, Δ-Bis(tiglate){(*R*)-2,2'-bis(diphenylphosphino)-1,1'-binaphthyl}ruthenium(II), [Ru^{II}(BINAP)(O₂CCMe=CHMe)₂]

Michael T. Ashby* and Masood A. Khan

Department of Chemistry, University of Oklahoma, 620 Parrington Oval, Room 208, Norman, Oklahoma 73019

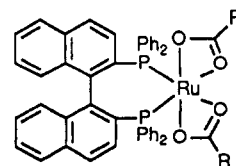
Jack Halpern*

Department of Chemistry, The University of Chicago, Chicago, Illinois 60637

Received October 25, 1990

The molecular structure of an active catalyst in the homogeneous asymmetric hydrogenation of tiglic acid has been determined by single-crystal X-ray crystallography. Bis(tiglate){(*R*)-2,2'-bis(diphenylphosphino)-1,1'-binaphthyl}ruthenium(II), (*R*)-1b, crystallizes in the monoclinic space group *P*2₁ with *Z* = 2, *a* = 12.709 (5) Å, *b* = 15.622 (5) Å, *c* = 11.289 (5) Å, β = 99.43 (4)°, *R* = 0.021, and *R*_w = 0.027. The tiglate ligands are η²-carboxylate-bound. The configuration at the metal is Δ, and the conformation of the seven-membered chelate ring is λ. No bonding interactions between the C=C bonds of the substrates and the metal center are found in the solid state. The coordination environment of the Ru atom in 1b in the solid state is essentially the same as that in noncoordinating solvents, as deduced by NMR spectroscopy. These results are consistent with the conclusion, on the basis of kinetic measurements previously reported, that if coordination of the C=C bond to Ru is a prerequisite to insertion into a Ru–H bond, then such coordination must occur after reaction with H₂.

We have recently reported the results of a study of the kinetics and mechanism of asymmetric hydrogenation of α,β-unsaturated carboxylic acids, catalyzed by ruthenium complexes derived from the precursor bis(acetato){(*R*)- or (*S*)-2,2'-bis(diphenylphosphino)-1,1'-binaphthyl}ruthenium(II) ([Ru^{II}(BINAP)(OAc)₂], 1a).¹ The results of this study, conducted in methanol solution, suggested a mechanism involving: (1) rapid equilibrium between 1 and

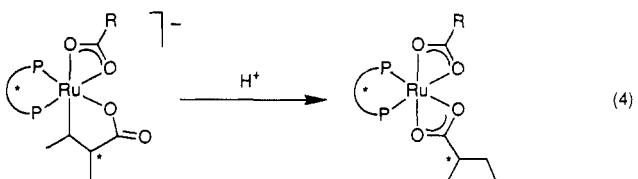
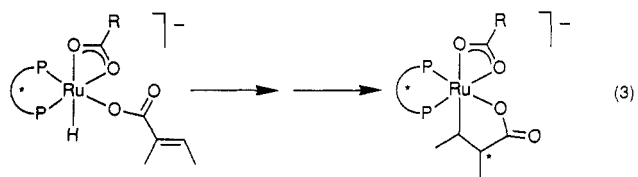
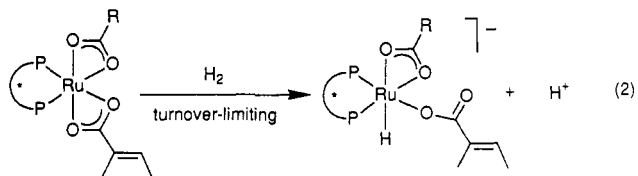
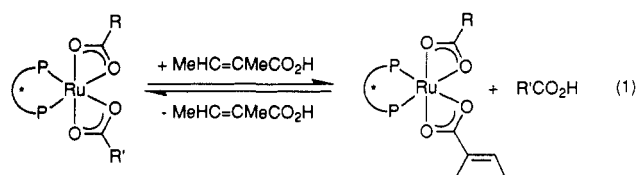


R = CH₃ (1a)
R = C(CH₃)=CHCH₃ (1b)
R = C(CH₃)₃ (1c)

(1) (a) Ashby, M. T.; Halpern, J. *J. Am. Chem. Soc.* 1991, 113, 589. (b) For a general review of asymmetric catalysis by BINAP complexes, see: Noyori, R.; Takaya, H. *Acc. Chem. Res.* 1990, 23, 345.

the substrate, (2) heterolytic splitting of H₂ to give a ruthenium–dicarboxylate–monohydride species, (3) insertion

Scheme I



of the C=C bond of the substrate into the Ru-H bond to give a five-membered heterometallacyclic species (note that this could be a multistep reaction), and (4) protonolysis of the Ru-C bond to regenerate the ruthenium-dicarboxylate adduct (Scheme I, eqs 1-4). Evidence for the formulation of **1a,b** as having two carboxylate-bound tiglate ligands was provided by NMR spectroscopy. The temperature dependencies of their NMR spectra are solvent dependent. Thus, in CD₂Cl₂ solution, the acetate ligands and the phosphorus atoms of the BINAP ligand of **1a** remain magnetically equivalent down to -90 °C. However, in methanol solution, the NMR of **1a,b** exhibit dynamic behavior. For each complex the two carboxylate ligands and the two phosphorus atoms of the BINAP ligand were found to be magnetically equivalent on the NMR time scale at room temperature by ¹H and ³¹P NMR spectroscopy. **1a**: ¹H NMR (CD₃OD, 20 °C), δ 1.71 (s, 6 H, OCCH₃), 6.1-8.0 (m, aromatic protons); ³¹P{¹H} (CD₃OD, 20 °C), δ 65.4 (s). **1b**: ¹H NMR (CD₃OD, 20 °C), δ 1.56 (s, 6 H, OC(CH₃)=C(H)(CH₃)), 1.62 (d, 6 H, ³J_{HH} = 4.5 Hz, OC(CH₃)=C(H)(CH₃)), 6.1-8.0 (m, aromatic and vinyl protons); ³¹P{¹H} (CD₃OD, 20 °C), δ 65.4 (s). However, neither the acetate ligands nor the phosphorus atoms of the BINAP ligand of **1a** remain magnetically equivalent at -80 °C: ¹H NMR (CD₃OD, -80 °C), δ 1.65 (s, 3 H, OCCH₃), 1.73 (s, 3 H, OCCH₃), 6.1-8.0 (m, aromatic protons); ³¹P{¹H} (CD₃OD, -80 °C), δ 65.63, 65.18 (³J_{PP} = 46 Hz). The molecular structure of **1b** in methanol at -80 °C is similar to that of **1a**: ³¹P{¹H} (CD₃OD, -80 °C), δ 66.18, 65.70 (³J_{PP} = 46 Hz). Thus, there is no evidence to suggest that the C=C bond of **1b** is coordinated to the metal.

The structures of **1a,b** in methanol are at variance with the solid-state structure of the pivalate derivative, **1c**,

Table I. Crystallographic Data for Δ-*R*-**1b** at -110 °C^a

formula	C ₅₄ H ₄₆ O ₄ P ₂ Ru
fw	921.98
space group	P2 ₁ (No. 4)
cell dimens	
<i>a</i> , Å	12.709 (5)
<i>b</i> , Å	15.622 (5)
<i>c</i> , Å	11.289 (5)
β, deg	99.43 (4)
<i>V</i> , Å ³	2211.0 (<i>Z</i> = 2)
<i>d</i> _{calcd} , g cm ⁻³	1.38
cryst shape	rectangular prism
cryst dimens, mm	0.13 × 0.28 × 0.35
abs coeff, cm ⁻¹	4.6
data collcn range, deg	3-55
no. of unique data	6520
no. of data used (<i>I</i> > 2σ(<i>I</i>))	5939
<i>R</i>	0.021
<i>R</i> _w	0.027
GOF	1.143
largest shift/esd, final cycle	0.2

^aThe standard deviation of the least significant figure is given in parentheses in this and subsequent tables. $R = \sum ||F_o| - |F_c|| / \sum |F_o|$, $R_w = [\sum w(|F_o| - |F_c|)^2 / \sum w|F_o|^2]^{1/2}$, and $GOF = [\sum (w(|F_o| - |F_c|)^2 / (m - n))]^{1/2}$.

which exhibits approximate *C*₂ molecular symmetry.² The solvent appears to affect the molecular structures (or rate of averaging of the structures) of **1a,b** in solution, perhaps by serving as an auxiliary ligand. In this paper we report the results of our determination of the crystal and molecular structure of **1b** in the solid state by X-ray crystallography.

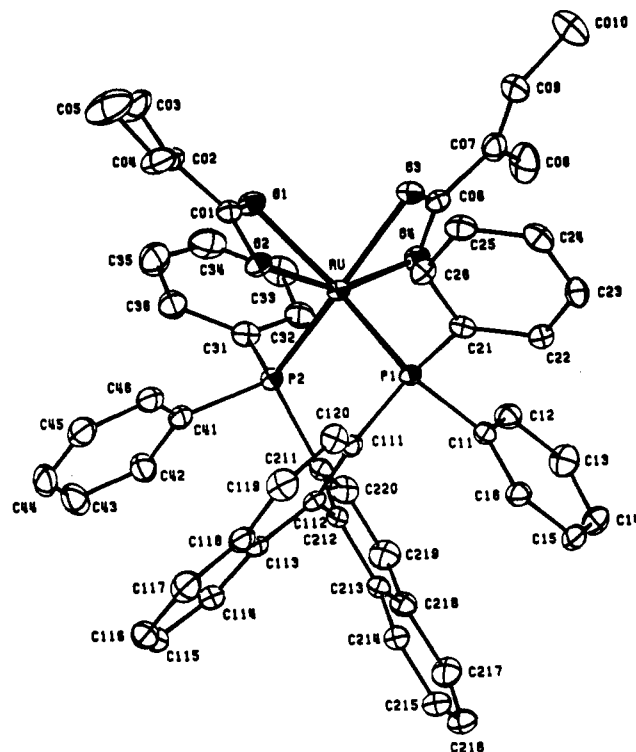
Results and Discussion

The impetus for determining the solid-state structure of **1b** was implication of the latter in the mechanism of catalytic asymmetric hydrogenation of tiglic acid.^{1a} By NMR spectroscopy in methanol, the symmetry of **1b**, in contrast to that in the noncoordinating solvent CD₂Cl₂, was found to be less than the *C*₂ symmetry expected for the simple pseudooctahedral formulation of [Ru(BINAP)(O₂CR)₂]. This serves as the basis for formulating **1** in methanol as a solvate. Our proposal that the tiglate ligands of **1b** are bound via their carboxyl groups in methanol, rather than the tiglate C=C bonds, was based on the similarities of the variable-temperature NMR spectra of **1b** and the acetate analogue **1a**. However, two questions remaining after these studies were (1) whether or not a static NMR spectrum had been achieved at the low-temperature limit of CH₂Cl₂ (-90 °C) and (2) what is the molecular structure of the 1-solvate complex that apparently is formed in methanol. In an attempt to address these questions that bear on the intimate mechanism illustrated in reactions 1-4, we grew crystals of **1b** from a methanol solution. The ¹H NMR spectrum of crystals of **1b** dissolved in CDCl₃ demonstrated the crystalline material did not contain any solvent of cocrystallization. The results of a single-crystal X-ray diffraction study of *R*-**1b** are summarized in the ORTEP drawings of Figures 1 and 2 and in the lists of crystallographic data and atomic fractional coordinates of Tables I and II.

The crystallographic results reveal that both of the tiglate ligands of **1b** are η²-bound to the ruthenium atom via their carboxylate groups. Accordingly, the metal is in a pseudooctahedral coordination environment, surrounded by three bidentate ligands. The known absolute configuration of the *R*-BINAP ligand allows the absolute configuration of *R*-**1b** to be deduced directly. Confirmation was

Table II. Atomic Coordinates for Δ -R-1b

atom	x	y	z
Ru	0.85608 (1)	0.00000 (0)	0.13009 (1)
P(1)	0.72520 (4)	-0.08685 (4)	0.04923 (5)
P(2)	0.75970 (5)	0.05727 (4)	0.25716 (5)
O(1)	1.0054 (1)	0.0476 (1)	0.2357 (2)
O(2)	0.9487 (1)	-0.0828 (1)	0.2539 (1)
O(3)	0.9521 (1)	-0.0139 (1)	-0.0132 (1)
O(4)	0.8380 (1)	0.0911 (1)	-0.0117 (1)
C(O1)	1.0221 (2)	-0.0258 (2)	0.2792 (2)
C(O2)	1.1260 (2)	-0.0465 (2)	0.3555 (2)
C(O3)	1.2002 (2)	0.0269 (3)	0.3893 (3)
C(O4)	1.1477 (2)	-0.1281 (3)	0.3826 (3)
C(O5)	1.2524 (3)	-0.1618 (3)	0.4469 (5)
C(O6)	0.9116 (2)	0.0553 (2)	-0.0590 (2)
C(O7)	0.9473 (2)	0.0946 (2)	-0.1656 (2)
C(O8)	0.8935 (3)	0.1754 (2)	-0.2139 (3)
C(O9)	1.0234 (2)	0.0546 (3)	-0.2121 (3)
C(O10)	1.0678 (4)	0.0828 (4)	-0.3215 (3)
C(11)	0.6032 (2)	-0.0529 (2)	-0.0502 (2)
C(12)	0.5963 (2)	0.0290 (2)	-0.0981 (2)
C(13)	0.5026 (2)	0.0550 (2)	-0.1740 (3)
C(14)	0.4189 (2)	-0.0012 (3)	-0.2018 (2)
C(15)	0.4258 (2)	-0.0840 (2)	-0.1551 (2)
C(16)	0.5175 (2)	-0.1092 (2)	-0.0784 (2)
C(21)	0.7802 (2)	-0.1683 (2)	-0.0397 (2)
C(22)	0.7327 (2)	-0.1916 (2)	-0.1561 (2)
C(23)	0.7847 (2)	-0.2472 (2)	-0.2231 (2)
C(24)	0.8840 (2)	-0.2803 (2)	-0.1759 (2)
C(25)	0.9317 (2)	-0.2577 (2)	-0.0612 (2)
C(26)	0.8810 (2)	-0.2015 (2)	0.0066 (2)
C(31)	0.8094 (2)	0.1679 (2)	0.2750 (2)
C(32)	0.7946 (2)	0.2255 (2)	0.1797 (2)
C(33)	0.8458 (2)	0.3043 (2)	0.1905 (3)
C(34)	0.9151 (3)	0.3254 (2)	0.2940 (3)
C(35)	0.9343 (2)	0.2665 (2)	0.3867 (3)
C(36)	0.8810 (2)	0.1887 (2)	0.3784 (3)
C(41)	0.7624 (2)	0.0250 (2)	0.4140 (2)
C(42)	0.7043 (2)	0.0740 (2)	0.4844 (2)
C(43)	0.7019 (3)	0.0513 (2)	0.6030 (3)
C(44)	0.7571 (2)	-0.0197 (2)	0.6514 (2)
C(45)	0.8133 (2)	-0.0694 (2)	0.5816 (3)
C(46)	0.8166 (2)	-0.0465 (2)	0.4628 (2)
C(111)	0.6740 (2)	-0.1443 (2)	0.1703 (2)
C(112)	0.6104 (2)	-0.1018 (2)	0.2408 (2)
C(113)	0.5881 (2)	-0.1416 (2)	0.3484 (2)
C(114)	0.5336 (2)	-0.0978 (2)	0.4303 (2)
C(115)	0.5149 (2)	-0.1376 (3)	0.5340 (2)
C(116)	0.5447 (2)	-0.2225 (3)	0.5573 (2)
C(117)	0.5973 (3)	-0.2663 (2)	0.4810 (3)
C(118)	0.6228 (2)	-0.2267 (2)	0.3761 (2)
C(119)	0.6836 (2)	-0.2685 (2)	0.2995 (3)
C(120)	0.7098 (2)	-0.2289 (2)	0.2011 (2)
C(211)	0.6143 (2)	0.0589 (2)	0.2080 (2)
C(212)	0.5596 (2)	-0.0177 (2)	0.2035 (2)
C(213)	0.4451 (2)	-0.0186 (2)	0.1597 (2)
C(214)	0.3846 (2)	-0.0948 (2)	0.1535 (2)
C(215)	0.2769 (2)	-0.0937 (2)	0.1116 (3)
C(216)	0.2245 (2)	-0.0171 (2)	0.0716 (2)
C(217)	0.2814 (2)	0.0564 (2)	0.0742 (3)
C(218)	0.3931 (2)	0.0581 (2)	0.1197 (2)
C(219)	0.4519 (2)	0.1347 (2)	0.1278 (3)
C(220)	0.5591 (2)	0.1361 (2)	0.1717 (2)

Figure 1. ORTEP drawing of Δ -R-1b. Atoms are represented by thermal vibration ellipsoids at the 50% level, and the labeling scheme is defined. Hydrogen atoms have been omitted for clarity.Table III. Conformations of BINAP Ligands^a

compd	P-M-P'	ϕ_b	ϕ_a	ϕ'_a	ϕ'_b	ϕ'_c
[Ru(R-BINAP)(O ₂ CC(CH ₃)=CHCH ₃) ₂] (1b)	93.2	-74	12	-7	43	72
[Ru(S-BINAP)(O ₂ CC-(CH ₃) ₂) ₂] (1c)	90.6	67	-10	3	-33	-51
[Ru(S-BINAP)(Cl)(C ₆ H ₆)]BF ₄ (2)	91.4	81	-13	-31	-4	-71
[Rh(R-BINAP)(nbd)]ClO ₄ (3)	91.8	-74	8	7	56	58
[Rh(R-BINAP) ₂]ClO ₄ ^b (4)	86.3	-66	4	-12	-39	-56
[(Rh(R-BINAP)) ₃ (OH) ₂]ClO ₄ (5)	88.6	-67	11	11	27	31
	88.1	-70	9	10	20	33
	89.1	-69	11	11	30	35

^a P-M-P' = the intra-BINAP angle; ϕ_b = the C2-C1-C1'-C2' torsion angle between the binaphthyl rings; ϕ_a = ϕ'_a = the torsional angle between the best-fit plane containing the axially oriented phenyl ring and the M-P bond; ϕ_b = ϕ'_b = the torsional angle between the best-fit plane containing the equatorially oriented phenyl ring and the M-P bond.
^b The molecule exhibits crystallographic 2-fold symmetry.

Ru-O distances are not equivalent; the two Ru-O bonds that are trans to the Ru-P bonds and cis to one another are longer (Ru-O_{av} = 2.195 (6) Å) than the two Ru-O bonds that are mutually trans (Ru-O_{av} = 2.121 (8) Å). This is consistent with the ligands' (P and O) relative trans influences.⁴ The structure of R-1b represents the sixth crystal structure of a metal complex of the BINAP ligand.⁵

provided by the higher *R* factor obtained for the alternate isomer (vide infra). The dissymmetry of the R-BINAP ligand imposes a λ conformation of the seven-membered P-Ru-P-C-C-C chelate ring. The Δ configuration of the three chelating ligands found about the Ru center of R-1b presumably is influenced by the stereochemical requirements of the R-BINAP ligand. Similarly, S-BINAP was used in the X-ray crystallographic study of S-1c, wherein the seven-membered chelate ring adopts a δ conformation and a Λ configuration was found at the metal.

The Ru-P distances of 1b are equivalent within experimental error (2.222 (2) Å) and are short compared to related Ru-P distances (2.20–2.45 Å).³⁴ However, the four

(3) (a) Skapski, A. C.; Troughton, P. G. H. *J. Chem. Soc., Chem. Commun.* 1968, 1230. (b) LaPlaca, S. J.; Ibers, J. A. *Inorg. Chem.* 1965, 4, 778. (c) Bergbreiter, D. E.; Bursten, B. E.; Bursten, M. S.; Cotton, F. A. *J. Organomet. Chem.* 1981, 205, 407. (d) Clark, G. R.; Grundy, K. R.; Harris, R. O.; James, S. M.; Roper, W. R. *J. Organomet. Chem.* 1975, 90, C37.

(4) Cotton, F. A.; Wilkinson, G. *Advanced Inorganic Chemistry*; 5th ed.; John Wiley & Sons: New York, 1988; p 1300.

(5) (a) Masima, K.; Kusano, K.; Ohta, T.; Noyori, R.; Takaya, H. *J. Chem. Soc., Chem. Commun.* 1989, 1208. (b) Toriumi, K.; Ito, T.; Takaya, H.; Souchi, T.; Noyori, R. *Acta Crystallogr.* 1982, B38, 807. (c) Tani, K.; Yamagata, T.; Tatsuno, Y.; Yamagata, Y.; Tomita, K.; Akutagawa, S.; Kumobayashi, H.; Otsuka, S. *Angew. Chem., Int. Ed. Engl.* 1985, 24, 217. (d) Yamagata, T.; Tani, K.; Tatsuno, Y.; Saito, T. *J. Chem. Soc., Chem. Commun.* 1988, 466. (e) Kawano, H.; Ishii, Y.; Kodama, T.; Saburai, M.; Uchida, Y. *Chem. Lett.* 1987, 1311.

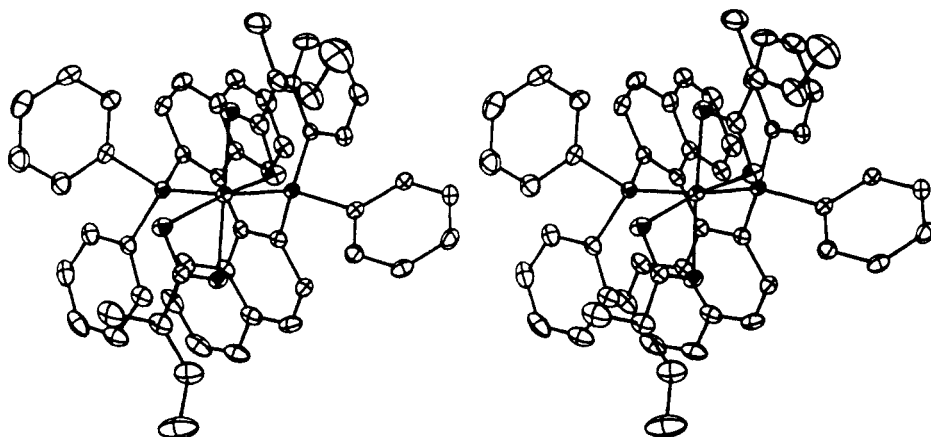


Figure 2. Stereoscopic view of Δ -*R*-1b, illustrating the orientation of the *R*-BINAP ligand.

Table III compares the conformations of the BINAP ligands in these complexes.⁶ The bite angle of the BINAP ligand ranges from 86 to 93°, with 1b defining the upper limit. The dihedral angles between the naphthyl rings of the BINAP ligands fall within a relatively narrow arc of 66–81°, with 1b again defining the upper limit. The latter two structural parameters are related because of the rigid nature of the backbone of the BINAP ligand. The other structural features of 1b are comparable to those of 1c.² The relative orientations of the phenyl rings of bidentate bis(diphenylphosphine) ligands are of some interest, since they define the steric topology about the metal. The seven-membered heterometallacyclic ring formed by the chelating BINAP ligand is significantly skewed. The effect of the latter is to orient two of the phenyl groups axially and the other two phenyl groups equatorially with respect to the P–Ru–P plane.⁷ The rotational orientations of the axial and equatorial phenyl groups are defined in Table III as their torsional orientations to corresponding P–Ru bonds. It may be deduced from the structural data of Table III that the rotational orientations of the phenyl groups of the BINAP ligands are comparable in those structures whose coordination spheres exhibit approximate C_2 symmetry about the coordination sphere of the metal (1b, c, 3–5); viz., the axial phenyl groups are coplanar with the M–P bonds, whereas the equatorial phenyl groups are rotated by ca. 45°. It is noteworthy that the rotational orientations of the phenyl groups of 2, the only compound of Table III that, by virtue of its different coligands, does not have approximate C_2 symmetry at the metal center, are different from those of the other compounds of Table III. This point may be relevant to the stereochemical role of the BINAP ligand in the catalysis of hydrogenation of α,β -unsaturated carboxylic acids by 1, since subsequent intermediates are not likely to exhibit C_2 symmetry.

In conclusion, olefinic substrates typically bind to homogeneous hydrogenation catalysts via their C=C bonds;

however, coordination of the substrate in 1b appears to be entirely through the carboxyl groups. The absence of any significant contribution from C=C bond coordination in this adduct is supported by the similarities of the NMR spectra of 1a–c, the solid-state structures of 1a, c, and kinetic data. While the presence of small amounts of (C=C)-coordinated isomers of 1b cannot be ruled out, the high turnover rates makes it unlikely that the reaction with H_2 is due to such minor species. We conclude that if (as is likely) coordination of the C=C bond to Ru is a prerequisite to insertion into the Ru–H bond of a catalytic intermediate, then such coordination must occur *after* reaction with H_2 .

Experimental Section

Compound *R*-1b was prepared from *R*-1a as previously described.¹ All manipulations were carried out in a Vacuum Atmospheres glovebox under a N_2 atmosphere. Spectroscopic grade methanol was dried by successive distillation from sodium under argon.

Crystallographic Data for *R*-1b. Yellow crystals were grown from a saturated methanol solution of *R*-1b by slow evaporation of the solvent in a glovebox. A crystal measuring $0.13 \times 0.28 \times 0.35$ mm was mounted and X-ray data were collected at $-110^\circ C$ with an Enraf-Nonius diffractometer using monochromated Mo $K\alpha$ radiation ($\lambda = 0.71069 \text{ \AA}$) and methods standard in this laboratory.⁹ The crystallographic data are summarized in Table I. Automatic centering, indexing, and least-squares routines gave the cell dimensions $a = 12.709 (5) \text{ \AA}$, $b = 15.622 (5) \text{ \AA}$, $c = 11.289 (5) \text{ \AA}$; $\alpha = \gamma = 90^\circ$, and $\beta = 99.43 (4)^\circ$. A trial data set showed the cell to be monoclinic and the space group to be $P2_1$ or $P2_1/m$. The noncentrosymmetric space group $P2_1$ was consistent with the optically active complex. The data were collected and corrected for Lorentz and polarization effects; however, no absorption correction was applied, since it was judged to be negligible. The structure was solved by the heavy-atom method using the SHELX-76 program.¹⁰ Neutral scattering factors were used for all atoms.¹¹ Initial refinement of all non-hydrogen atoms with anisotropic thermal parameters gave an R factor of 0.033. The difference Fourier map at this stage revealed all the hydrogen atoms with peak heights between 0.6 and $0.7 e \text{ \AA}^3$. All the hydrogen atoms were refined with isotropic temperature factors to give $R = 0.021$ and $R_w = 0.027$. The absolute configuration of the complex was tested by inverting the coordinates of the atoms and refining the alternate isomer to give $R = 0.025$ and $R_w = 0.033$. An R factor ratio test indicated that the alternative stereochemistry could be rejected at the 99.9% confidence level.¹² The final positional

(6) The atomic fractional coordinates for one of the compounds are not available from the Cambridge Data Files.^{6a}

(7) (a) McCulloh, B.; Halpern, J.; Thompson, M. R.; Landis, C. R. *Organometallics* 1990, 9, 1392 and references therein. (b) Koenig, K. E.; Sabacky, M. J.; Bachman, G. L.; Christophel, W. C.; Barnstorff, H. D.; Friedman, R. B.; Knowles, W. S.; Stults, B. R.; Vineyard, B. D.; Weinkauff, D. J. *Ann. N.Y. Acad. Sci.* 1980, 333, 16. (c) Bosnich, B.; Roberts, N. K. *Adv. Chem. Ser.* 1982, No. 196, 337. (d) Oliver, J. D.; Riley, D. P. *Organometallics* 1983, 2, 1032.

(8) Taking into account the handedness of the BINAP ligands, the phenyl groups of 1b, c, 3, and 5 (the metal complexes that are ligated by one BINAP ligand and that exhibit approximate C_2 symmetry) are rotated in the same sense, whereas, the phenyl groups of 4 (the only metal complex ligated by two BINAP ligands and exhibiting approximate C_2 symmetry) are rotated in the opposite sense.

(9) Khan, M. A.; Taylor, R. W.; Lehn, J. M.; Dietrich, B. *Acta Crystallogr.* 1988, C44, 1928.

(10) SHELX-76. Program for Crystal Structure Determination; University of Cambridge: Cambridge, England, 1976.

(11) *International Tables for X-ray Crystallography*; Kynoch Press: Birmingham, England, 1974; Vol. IV, pp 99, 149.

parameters for all of the non-hydrogen atoms are given in Table II.

Acknowledgment. M.T.A. thanks the University of Oklahoma Department of Chemistry, and J.H. thanks the National Science Foundation (Grant CHE 8808446) for

their support. The loan of ruthenium by the Johnson-Matthey Co. and the gift of BINAP by Hoffmann-La Roche Inc. are gratefully acknowledged.

Supplementary Material Available: Tables of atomic coordinates of the hydrogen atoms and anisotropic thermal parameters of the non-hydrogen atoms (5 pages); a table of observed and calculated structure factor amplitudes (35 pages). Ordering information is given on any current masthead page.

(12) Hamilton, W. C. *Acta Crystallogr.* 1965, 18, 502.

Multidentate Lewis Acids. Adducts of Monodentate and Bidentate Titanium Trichloroalkoxides with Ketones

Benoit Bachand¹ and James D. Wuest*

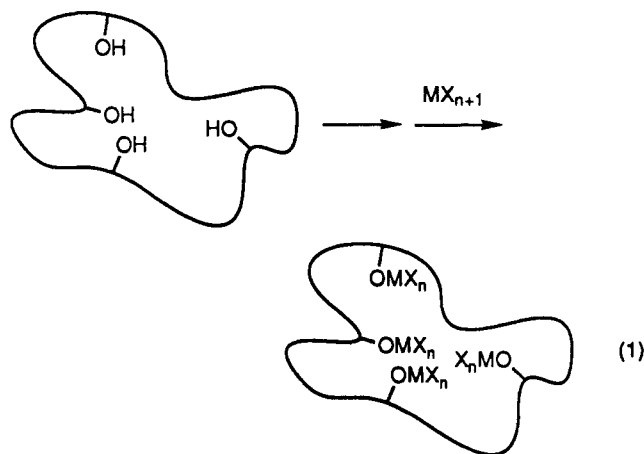
Département de Chimie, Université de Montréal, Montréal, Québec, H3C 3J7 Canada

Received January 25, 1991

Like TiCl_4 , titanium trichloroisopropoxide (4) is a strong Lewis acid able to form 1:2 adducts with ketones. Low-temperature ^1H and ^{13}C NMR spectra indicate that these adducts adopt a *mer* octahedral geometry. Exchange of free and bound pinacolone occurs by a dissociative mechanism with $\Delta G^\ddagger_{219} = 9.2$ kcal/mol. Potentially bidentate titanium trichloroalkoxides 19–21 can be prepared by treating the bis(trimethylsilyl) ethers of *trans*-1,2-cyclohexanediols with 2 equiv of TiCl_4 . Compounds 19–21 form crystalline 1:2 ketone adducts even in the presence of excess ketone. An X-ray crystallographic study has shown that the close proximity of the OTiCl_3 groups favors symmetric adducts 30 ($\text{X} = \text{Cl}$) with bridging chlorides, not adducts 31 with bridging, doubly activated carbonyl groups. Similar chloride-bridged structures are adopted in solution. Low-temperature ^1H and ^{13}C NMR spectra establish that unsymmetric 1:3 adducts 36 ($\text{X} = \text{Cl}$) are formed in solution in the presence of additional ketone. Symmetrization of the 1:3 pinacolone complex derived from bidentate titanium trichloroalkoxide 21 occurs by a normal dissociative mechanism with $\Delta G^\ddagger_{223} = 10.4$ kcal/mol. Since this process is slower than exchange in 1:2 adducts of monodentate analogue 4, symmetric intermediates or transition states 38 ($\text{X} = \text{Cl}$) with a single bridging carbonyl oxygen do not offer a low-energy intramolecular pathway for exchange. Slow exchange in the 1:3 adduct provides evidence that the two OTiCl_3 groups in compounds 19–21 cooperate by forming a single chloride bridge that enhances the Lewis acidity of one site at the expense of the other.

The unique ability of well-designed multidentate Lewis acids to recognize, bind, transport, and activate basic guests is attracting the attention of a growing number of chemists.^{2,3} We have contributed to the study of multidentate Lewis acids by showing that they can be made conveniently

by adding metal salts MX_{n+1} to compounds containing hydroxyl groups or similar sites suitably oriented by an organic framework (eq 1).³ An important practical goal



of this work is to devise bidentate Lewis acids 1 that can activate carbonyl compounds by forming complexes 2 in which the substrate is cooperatively bound (eq 2). These complexes promise to be unusually susceptible to nucleophilic additions,⁴ and their rigid orientation should help

(1) Fellow of the Natural Sciences and Engineering Research Council of Canada, 1986–1990. Fellow of the Ministère de l'Éducation du Québec, 1990–1991.

(2) For recent work on multidentate Lewis acids, see: Nadeau, F.; Simard, M.; Wuest, J. D. *Organometallics* 1990, 9, 1311–1314. Narasaka, K.; Sakurai, H.; Kato, T.; Iwasawa, N. *Chem. Lett.* 1990, 1271–1274. Dohmeier, C.; Mattes, R.; Schnöckel, H. *J. Chem. Soc., Chem. Commun.* 1990, 358–359. Kaufmann, D.; Boese, R. *Angew. Chem., Int. Ed. Engl.* 1990, 29, 545–546. Chujo, Y.; Tomita, I.; Saegusa, T. *Macromolecules* 1990, 23, 687–689. Layh, M.; Uhl, W. *Polyhedron* 1990, 9, 277–282. Jurkschat, K.; Rühlemann, A.; Tzschach, A. *J. Organomet. Chem.* 1990, 381, C53–C56. Kelly, T. R.; Meghani, P. *J. Org. Chem.* 1990, 55, 3684–3688. Tamao, K.; Hayashi, T.; Ito, Y.; Shiro, M. *J. Am. Chem. Soc.* 1990, 112, 2422–2424. Newcomb, M.; Horner, J. H.; Blanda, M. T.; Squattrito, P. *J. Ibid.* 1989, 111, 6294–6301. Jurkschat, K.; Kuivila, H. G.; Liu, S.; Zubieta, J. A. *Organometallics* 1989, 8, 2755–2759. Katz, H. E. *J. Org. Chem.* 1989, 54, 2179–2183. Schmidbaur, H.; Öller, H.-J.; Wilkinson, D. L.; Huber, B.; Müller, G. *Chem. Ber.* 1989, 122, 31–36. Jung, M. E.; Xia, H. *Tetrahedron Lett.* 1988, 29, 297–300. Kaufmann, D. *Chem. Ber.* 1987, 120, 901–905. Khan, M. A.; Peppe, C.; Tuck, D. G. *Organometallics* 1986, 5, 525–530.

(3) (a) Phan Viet, M. T.; Sharma, V.; Wuest, J. D. *Inorg. Chem.*, in press. (b) Bélanger-Gariépy, F.; Hoogsteen, K.; Sharma, V.; Wuest, J. D. *Inorg. Chem.*, in press. (c) Bachand, B.; Bélanger-Gariépy, F.; Wuest, J. D. *Organometallics* 1990, 9, 2860–2862. (d) Sharma, V.; Simard, M.; Wuest, J. D. *Inorg. Chem.* 1991, 30, 579–581. (e) Galeffi, B.; Simard, M.; Wuest, J. D. *Ibid.* 1990, 29, 955–958. (f) Galeffi, B.; Simard, M.; Wuest, J. D. *Ibid.* 1990, 29, 951–954.

(4) Wuest, J. D.; Zacharie, B. *J. Am. Chem. Soc.* 1985, 107, 6121–6123.